J Therm Anal Calorim (2012) 107:477–481
DOI 10.1007/s10973-011-1544-3

The phase diagram of $CsNO_3$–$RbNO_3$

S. Wacharine · D. Hellali · H. Zamali · J. Rogez · M. Jemal

Received: 12 January 2011 / Accepted: 30 March 2011 / Published online: 1 May 2011

Abstract The phase transitions of $RbNO_3$ and the binary phase diagram of (Cs,Rb)NO_3 were investigated at atmospheric pressure, using simultaneous direct and differential thermal analysis, μDTA and DSC techniques. A fourth phase transition of $RbNO_3$ has been observed at temperature near the melting point. The phase diagram of this system is characterised by a eutectic, two eutectoid and an azeotropic-like invariants. Three limited solid solutions and two continuous solid solutions have been detected at low temperature.

Keywords Phase diagram · Phase transitions of $RbNO_3$ · Thermal analysis techniques · Eutectic, eutectoid and azeotropic-like invariants · Solid solutions

Introduction

Molten salt systems involving alkali nitrates are widely used in several fields (technical processes, energy storage, electrochemical and chemical applications…). Thus, knowledge of their thermodynamic properties and their phase diagrams contributes to give information for their use.

S. Wacharine · D. Hellali · H. Zamali (✉) · M. Jemal
Applied Thermodynamics Laboratory, Chemistry Department, Faculty of Science, Tunis El Manar University, 2092 Tunis El Manar, Tunisie
e-mail: hmida.Zamali@fst.rnu.tn

J. Rogez
Institut Matériaux Microélectronique Nanosciences de Provence (IM2NP), UMR 6242 CNRS, Paul Cézanne University, Avenue Escadrille Normandie-Niémien, 13397 Marseille Cedex 20, France

Complete phase diagram of the $CsNO_3$–$RbNO_3$ system has never been reported in literature. Wallerant [1], Blidin [2] (Fig. 1a) studied only the liquidus in a range of composition close to $RbNO_3$. Protsenko and Belova [3] considered this system as forming a continuous series of solid solutions with a minimum at 290 °C. Khovokov and Eumoe [4] (Fig. 1b), working on the liquid–solid equilibria of this system, reported the presence of a minimum at 80 mol.% $RbNO_3$ and 288 °C. Secco and Secco [5] (Fig. 1c), showed an incomplete phase diagram and estimated the limit of the stability domains of the solid phases by discontinuous lines but indexation they reported is not coherent.

Moreover, there is a divergence concerning the temperature transformations of pure nitrates and the number of polymorphic varieties of $RbNO_3$. In the majority of the literature data, $RbNO_3$ exhibits at atmospheric pressure four polymorphic forms between room temperature until melting point, which are as follows:

$$IV(\alpha) \rightarrow III(\beta) \rightarrow II(\gamma) \rightarrow I(\delta)$$

The low temperature form, $RbNO_3$ (α), has a trigonal structure [6–10], $RbNO_3$ (β) is cubic [6–9, 11]. There are some controversies about the structure of $RbNO_3$ (γ). Three different suggestions were reported: trigonal [12–14], tetragonal [6] and cubic [7, 11]. $RbNO_3$ (δ) has been reported to have a cubic structure [6, 7, 9, 11].

According to several authors, the temperature of the first transition (α/β) lies in the 160–167 °C range [6, 7, 15–24], the β/γ transition appears in 218–229 °C range [6, 7, 15–23]. Freeman and Anderson [24] reported 236 °C for that transition, whereas the third one (γ/δ), lies in the 280.5–291 °C range [6, 7, 15, 17–24].

Only Freeman and Anderson [24] reported in 1963 that $RbNO_3$ exhibits a fifth allotropic form (λ). According to these authors the fourth phase transition (δ/λ) appeared at

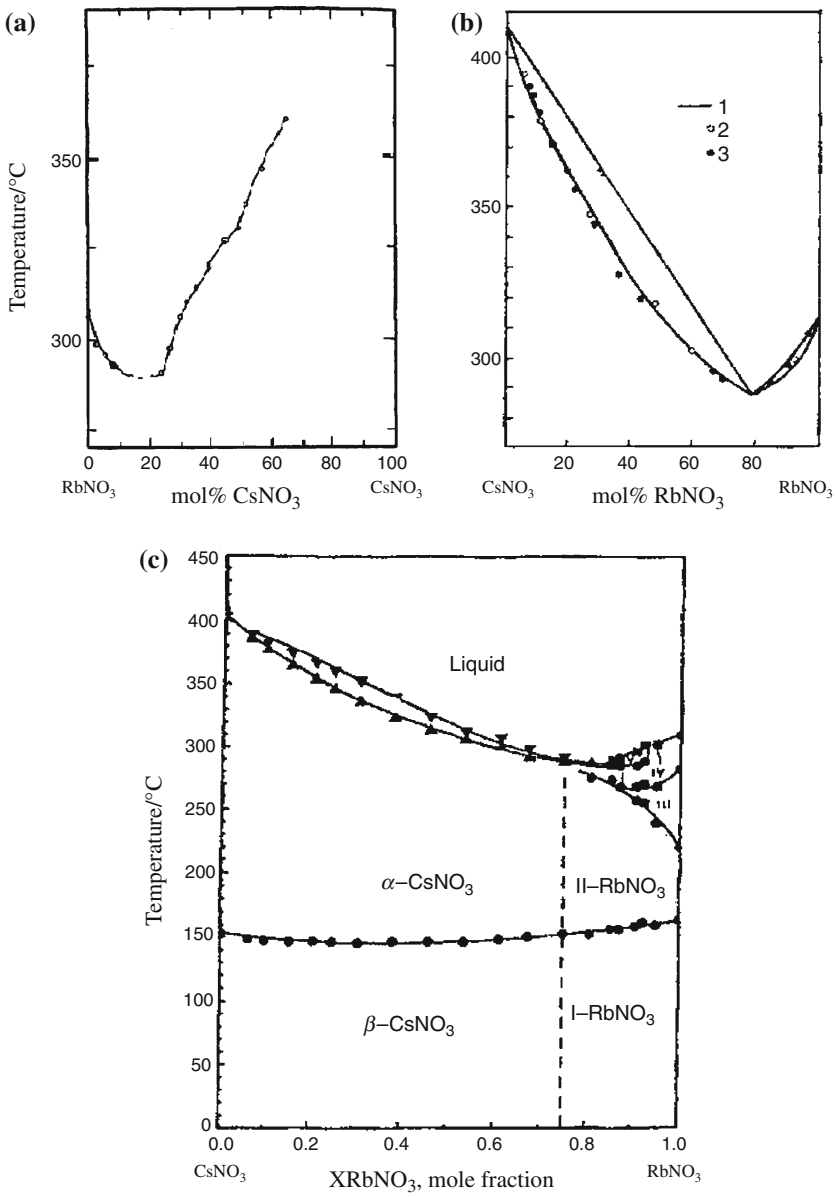

Fig. 1 Phase diagram of $(Cs,Rb)NO_3$ system reported by: **a** Blidin [2], **b** Khovostov and Eumoe [4] and **c** Secco and Secco [5]

302 °C and involved a very small heat change estimated as 209 J/mol.

In 1998, Chary and Reddy [10] reported an abrupt change in the conductivity of crystal $RbNO_3$ at a temperature close to the melting point. This suggested the existence of a new phase transition. This transition has not been mentioned in the previous published phase diagrams involving $RbNO_3$.

The melting point reported by several authors is in the range 310–317 °C [4, 6, 15–22, 25–30].

Enthalpy of the first transition ($\alpha \rightarrow \beta$) has been reported between 3715 and 4000 J/mol [5, 17, 22, 23, 31–34]. That of the second one ($\beta \rightarrow \gamma$) lies in 2321–3290 J/mol range [17, 22, 23, 31–34]. Values of the third transition ($\gamma \rightarrow \delta$) were in 958–1740 J/mol range [17, 22, 23, 31–34]. Whereas, the heat of melting lies in the range of 4600–5600 J/mol [5, 22, 35].

According to literature, $CsNO_3$ has two polymorphic forms at atmospheric pressure. At room temperature, $CsNO_3$ has a trigonal structure (α) [36, 37] which transforms into cubic one (β) in the range 151–161 °C [5, 15, 16, 18, 36, 38–49]. Most of the melting temperatures are in the range 404–411.7 °C [4, 5, 15, 25–28, 38–40, 42–44, 47–52]. Bol'shakov et al. [46, 47] reported the value of 414 °C, whereas Kleppa and McCarty [29] and Shenkin [30] gave 417 °C.

Experimental

In order to precise at atmospheric pressure the number of polymorphic varieties of $RbNO_3$ we used a simultaneous direct and differential thermal analysis technique. The device was already described in details in previous works [38, 39, 53]. It consists of an Adamel-Lhomargyam furnace connected to a Setaram PRT 540 C regulator-programmer of temperature, that allows to select a cooling or a heating rate between 0.35 and 10 °C min^{-1}. The furnace is provided with a metallic block with two symmetrical cavities for platinum crucibles of 3 cm^3 capacity. The external diameter of the block was a few millimetres smaller than the furnace, thus limiting the convection current around the test tubes, improving the heat transfer and making the thermal flow propagation homogeneous. Two thin-walled platinum crucibles were used with glove fingers for Chromel–Alumel thermocouples. The latter also act as crucible holders. Electrical and thermal isolation between the sample and the reference was ensured by two quartz tubes surrounding the crucibles. A (AOIP: P12) potentiometer connected to a direct current power source and to a highly sensitive "Keithley 191" multimeter was used to detect electromotive force from the sample thermocouple.

The phase transitions of $RbNO_3$ were detected using a μDTA device which has been described in a previous paper [54]. DSC measurements were performed using a Mettler-Toledo DSC822e. Platinum sample pans were used for these experiments.

DTA, μDTA and DSC devices were calibrated with high purity $NaNO_3$, KNO_3, Sn, Zn and In, respectively.

Heating and cooling rates were about 2 °C min^{-1} for the first cycle and they were reduced at 0.5°C min^{-1} for the next cycles and sometimes to about 0.37 °C min^{-1} in order to avoid the overlapping which was often encountered with the mixtures having molar composition in the range $0 \leq x_{CsNO_3} \leq 0.1$.

Accuracy of temperature measurements is about 1 °C for the DTA, μDTA and DSC. Accuracy of DSC enthalpies is about 5%.

For the study of $RbNO_3$ phase transitions, we used different purities: 99.99, 99.7 wt% from Aldrich Chemical Co. and 99.975 wt% from Alfa Aesar.

(Cs,Rb)NO_3 phase diagram was drawn using $CsNO_3$ and $RbNO_3$ 99.99 wt% purity (Aldrich Chemical Co). They were used without further purification, but dried for more than 24 h at 107 °C in an oven. The samples were prepared by intimately mixing various amounts of $CsNO_3$ and $RbNO_3$ in a platinum crucible. In order to get homogeneous mixtures without decomposition, the mixtures (2.5 g) were previously melted several times at a temperature a few degrees over the melting point.

Results and discussion

For $CsNO_3$, the solid state transition temperature is (156 ± 1) °C. Melting point is (409 ± 1) °C. These values are in the range of the most of the results published previously.

$RbNO_3$ exhibits four polymorphic phase transitions in the solid state. These transitions have been shown using different techniques and samples having 99.99, 99.975 and 99.7 wt% purity. The results are gathered in Table 1.

Considering certain purity, the temperature values of the transitions and the melting point are close to each other whatever the technique used. However, our results agree with those of literature, except for the (β/γ) transition $RbNO_3$ with 99.975 wt% purity. Measurements of this temperature exceed slightly the upper limit of the range of literature values, except the Freeman's value which is higher than our's (236 °C) but only the temperature of the fourth transition (δ/λ) of $RbNO_3$ with 99.99 wt% purity, is higher than the Freeman's value [24] (302 °C).

Moreover it should be noticed that this transition point (δ/λ) depends considerably on the purity of the nitrate. The temperature of this transition is near the melting point when the purity is high (99.975 and 99.99 wt%), and decreases when the purity decreases (99.7 wt%).

Values for melting point found in the present work for $RbNO_3$ ((313 ± 1) °C) are in good agreement with the literature results.

Enthalpies associated to these phase transitions and to the melting of $RbNO_3$ are gathered in Table 2.

It should be noticed that the heats involved in the four transitions and in fusion of the 99.7 wt% purity $RbNO_3$ are higher than those with the other purities (99.975 and 99.99 wt%).

The enthalpies of the first phase transition for $RbNO_3$ with 99.975 and 99.99 wt% purities are slightly less than the lower limit of the literature range. The enthalpies of the second and the third transitions are in good agreement with the literature values. However, the 99.99 wt% sample exhibit an enthalpy of the new phase transition higher than the value estimated by Freeman and Anderson [24].

Table 1 Temperatures of the solid–solid phase transitions and of the melting of $RbNO_3$

Technique	DTA	DSC	DTA	DSC	μDTA	DSC
Purity/wt%	99.99	99.99	99.975	99.975	99.7	99.7
T (α/β)/°C	166	164.6	164	163.7		164.1
T (β/γ)/°C	228	227.3	233.5	230.3	222	220.4
T (γ/δ)/°C	287	284.7	285	285.8	285.5	283.2
T (δ/λ)/°C	311	309.7	293	294.2	291	290.9
T_{fus}/°C	314	313.9	314.5	313.4	310	311.8

Table 2 Enthalpies of the solid–solid phase transitions and of melting of $RbNO_3$ at temperatures reported in Table 1 (5% accuracy)

Purity/wt%	$\Delta_{\alpha/\beta}H$/J/mol	$\Delta_{\beta/\gamma}H$/J/mol	$\Delta_{\gamma/\delta}H$/J/mol	$\Delta_{\delta/\lambda}H$/J/mol	$\Delta_{fus}H$/J/mol
99.99	3598.8	2520.3	1559.2	339.45	4375.21
99.975	3197.64	2358.6	1544.22	151.31	4135.72
99.7	3845.31	2797.06	1607.72	–	5604.43

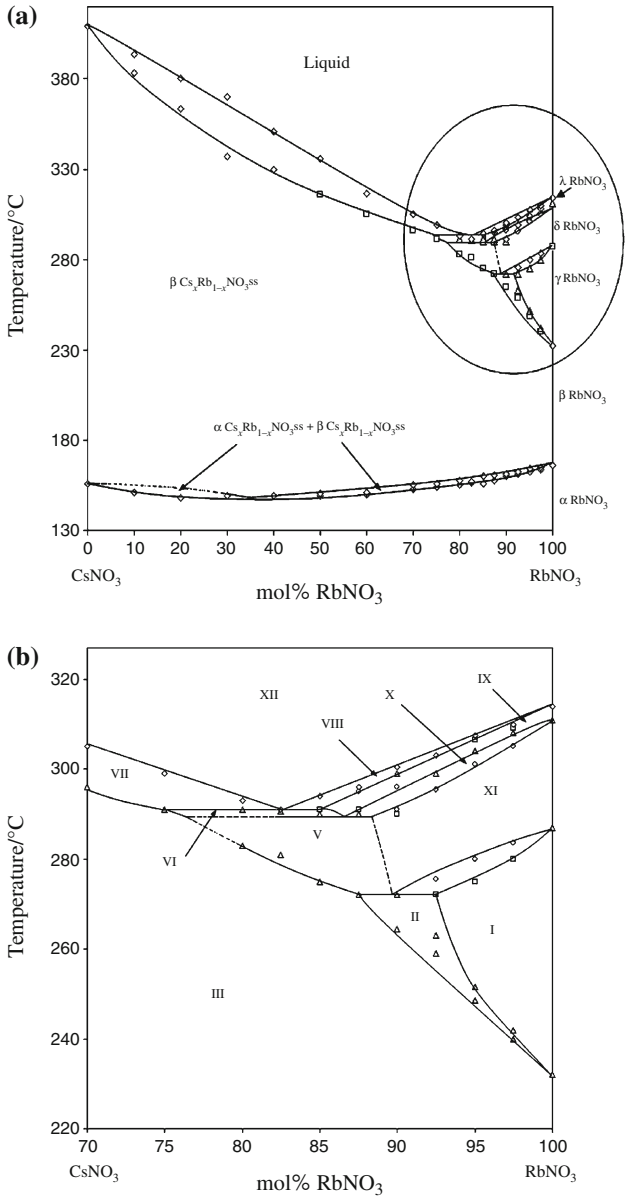

Fig. 2 **a** Phase diagram of the of $(Cs,Rb)NO_3$ system (this work). **b** Partial representation of the phase diagram of $(Cs,Rb)NO_3$ system (in the range 70–100 mol.% $RbNO_3$). *I*: $\gamma Cs_xRb_{1-x}NO_3$ ss, *II*: $\beta Cs_xRb_{1-x}NO_3$ ss + $\gamma Cs_xRb_{1-x}NO_3$ ss, *III*: $\beta Cs_xRb_{1-x}NO_3$ ss, *IV*: $\delta Cs_xRb_{1-x}NO_3$ ss + $\gamma Cs_xRb_{1-x}NO_3$ ss, *V*: $\beta Cs_xRb_{1-x}NO_3$ ss + $\delta Cs_xRb_{1-x}NO_3$ ss, *VI*: $\beta Cs_xRb_{1-x}NO_3$ ss + $\lambda Cs_xRb_{1-x}NO_3$ ss, *VII*: Liquid + $\beta Cs_xRb_{1-x}NO_3$ ss, *VIII*: Liquid + $\lambda Cs_xRb_{1-x}NO_3$ ss, *IX*: $\lambda Cs_xRb_{1-x}NO_3$ ss, *X*: $\delta Cs_xRb_{1-x}NO_3$ ss + $\lambda Cs_xRb_{1-x}NO_3$ ss, *XI*: $\delta Cs_xRb_{1-x}NO_3$ ss, *XII*: liquid

Attempts to measure the heat involved by that transition with (99.7 wt%) purity sample were not successful.

Concerning the heat of melting, one can notice that except for the $RbNO_3$ having the lower purity (99.7 wt%), our data are smaller.

Figure 2 shows the obtained phase diagram which is characterised by three reduced solid solutions, a eutectic point at 291 °C and 82.5 mol.% $RbNO_3$, corresponding to liquid = $\beta Cs_xRb_{1-x}NO_3$ ss + $\lambda Cs_xRb_{1-x}NO_3$ ss, a eutectic plateau at 291 °C, two eutectoid points at (87 mol.% $RbNO_3$, 290 °C) and at (89.5 mol.% $RbNO_3$, 272 °C), corresponding to $\lambda Cs_xRb_{1-x}NO_3$ ss = $\beta Cs_xRb_{1-x}NO_3$ ss + $\delta Cs_xRb_{1-x}NO_3$ ss and $\delta Cs_xRb_{1-x}NO_3$ ss = $\gamma Cs_xRb_{1-x}NO_3$ ss + $\beta Cs_xRb_{1-x}NO_3$ ss, respectively, an eutectoid plateau at 290 °C, an another eutectoid plateau at 272 °C, an azeotrope-like point at (35 mol.% $RbNO_3$, 148 °C) with the reaction $\beta Cs_xRb_{1-x}NO_3$ ss = $\alpha Cs_xRb_{1-x}NO_3$ ss and two solid solutions $\alpha Cs_xRb_{1-x}NO_3$ ss and $\beta Cs_xRb_{1-x}NO_3$ ss involving ($\alpha CsNO_3$ and $\alpha RbNO_3$) and ($\beta CsNO_3$ and $\beta RbNO_3$), respectively.

As a concluding remark, a fourth phase transition of $RbNO_3$ has been detected for the second time. The temperature of this transition depends considerably on the purity of the nitrate. The binary system caesium nitrate–rubidium nitrate studied at atmospheric pressure, by using a simultaneous direct and differential thermal analysis technique, showed a eutectic, two eutectoid points, a minimum and two continuous solid solutions.

References

1. Wallerant F. Binary systems formed by alkali metal nitrates. Bull Soc Min. 1905;28:206. Cited in Ref. 45.
2. Blidin VP. Reciprocal system of rubidium and cesium chlorides and nitrates. Izv Sektora Fiz Khim Anal Inst Obshch Neorg Khim Akad Nauk SSSR. 1953;23:233–40.
3. Protsenko PI, Belova ZI. Binary systems of calcium nitrate with the nitrates of the first and second group. Zh Neorg Khim. 1957;2:2617–20.
4. Khovokov IP, Eumoe AI. Solidus and liquidus curves of (Rb–Cs)NO_3 and (K–Cs)NO_3 systems. Zh Irikl Khim. 1974;47(5):1149–50.
5. Secco EA, Secco RA. Heats of solution/substitution in $TlNO_3$ and $CsNO_3$ crystals and in $RbNO_3$ and $CsNO_3$ crystals from heats of transition: the complete phase diagrams of $TlNO_3$–$CsNO_3$ and $RbNO_3$–$CsNO_3$ systems. J Phys Chem Solids. 2002;63:433–40.
6. Brown RN, McLaren AC. The thermal transformations in solid rubidium nitrate. Acta Cryst. 1962;15:974–6.

7. Shamsuzzoha M, Lucas BW. Polymorphs of rubidium nitrate and their crystallographic relationships. Can J Chem. 1988;66: 819–23.
8. Pohl J, Pohl D, Adiwidjaja G. Phase transition in rubidium nitrate at 346 K and structure at 296, 372, 413 and 437 K. Acta Cryst. 1992;B48:160–6.
9. Zhu B, Stjerna B, Mellander B-E. Cubic rubidium nitrate at room temperature. Solid State Commun. 1994;89(2):135–8.
10. Chary AS, Reddy SN. Effect of structural changes on DC ionic conductivity of rubidium nitrate single crystals. Phys Status Solidi B. 1998;208:349–52.
11. Lucas BW. Phase transitions and disorder in rubidium nitrate. Mater Sci Forum. 1988;27–28:95–8.
12. Finbak C, Hasselo O, Stromme LC. Polymorphs of rubidium nitrate and their crystallographic relationships. Z Phys Chem. 1937;B37:468. Cited in Ref. 7.
13. Salhotra PP, Subbarao EC, Venkateswarlu P. Polymorphism of rubidium nitrate. Phys Status Solidi. 1968;29:859–64.
14. Ahtee M, Hewat AW. Structures of the high temperature phases of rubidium nitrate. Phys Status Solidi. 1980;A58:525–31.
15. Ichikawa K, Matsumoto T. The heat capacities of lithium, sodium, potassium, rubidium and caesium nitrates in the solid and liquid states. Bull Chem Soc Jpn. 1983;56(7):2093–100.
16. Rao CNR, Rao KJ. Phase transitions in solids. Great Britain: Mc Graw-Hill Inc.; 1978. p. 17–37.
17. Mustajoki A. The specific heats and heats of transition of $RbNO_3$. Ann Acad Sci Fenn Ser A VI. 1958;9:3–16.
18. Plyshchev VE, Markina IB, Shklover LP. The diagrams of phase transformation of the binary systems obtained from rubidium and cesium nitrates with the nitrates of strontium and barium. Zh Neorg Khim. 1956;1:1613–8.
19. Hichri M, Favotto C, Zamali H, Feutelais Y, Legendre B, Sebaoun A, Jemal M. Diagramme de phases du système binaire $AgNO_3$–$RbNO_3$. J Therm Anal Calorim. 2002;69:509–18.
20. Protsenko PI, Grin'ko LS, Venerovskaya LN, Lyutsedarskii VA. Solid solutions of the potassium, rubidium//nitrite, nitrate system. J Appl Chem USSR. 1973;46:2568–71.
21. Cleavar B, Rhodes ER, Ubbelohde AR. Studies of phase transformations in nitrates and nitrites. I. Changes in ultra-violet absorption spectra on melting. Proc R Soc. 1963;A276:437–53.
22. Secco EA, Secco RA. Heats of solution/substitution in $TlNO_3$ and $RbNO_3$ crystals from heats of transition. The complete phase diagram of the $TlNO_3$–$RbNO_3$ system. J Phys Chem Chem Phys. 1999;1:5011–6.
23. Charsley EL, Laye PG, Markham HM, Hill JO, Berger B, Griffiths TT. Determination of the equilibrium temperatures and enthalpies of the solid–solid transitions of rubidium nitrate by differential scanning calorimetry. Thermochim Acta. 2008;469:65–70.
24. Freeman EL, Anderson DA. Physical transitions of the alkali metal nitrates as revealed by differential thermal analysis. Nature. 1963;199(4888):63–4.
25. Diogenov GG, Kirillova VF. K, Rb//F, NO_3 and Rb, Cs//F, NO_3 systems. Zh Neorg Khim. 1983;28(9):2384–8.
26. Denielou L, Petitet JP, Tequi C, et Sirousse-Zia D. Masse volumique et coefficient de dilatation des nitrates alcalins fondus et de leurs mélanges. J Chim Phys. 1977;74(2):247–8.
27. Diogenov GG, Sarapulova IF. The Cs, Li, Na//NO_3 and Li, Na, Rb//NO_3 systems. Russ J Inorg Chem. 1965;10(8):1052–4.
28. Sirousse-Zia D, Denielou L, Petitet JP, Tequi C. Complément à l'étude thermodynamique de sels fondus à anion polyatomique. J Phys Lett. 1977;15(T 38):L61–3.
29. Kleppa OJ, McCarty FG. Heats of fusion of the monovalent nitrates by high-temperature reaction calorimetry. J Chem Eng Data. 1963;8(3):3331–2.
30. Shenkin YS. Fusion diagrams for binary systems comprising alkali metal nitrates and chlorides. Zh Fiz Khim. 1980;54(5):1330–2.
31. Rao KJ, Rao CNR. Crystal structure transformations of alkali sulphates, nitrates and related substances: thermal hysteresis in reversible transformations. J Mater Sci. 1966;1:238–48.
32. Arell A, Varteva M. Transition energies and temperatures of $RbNO_3$ at the transitions II = III and III = IV. Ann Acad Sci Fenn Ser A VI. 1961;88:8.
33. Höhne GWH, Breuer KH, Eysel W. Differential scanning calorimetry: comparison of power compensated and heat flux instruments. Thermochim Acta. 1983;69:145–51.
34. Höhne GWH, Eysel W, Breuer KH. Results of a round robin experiment on the calibration of differential scanning calorimeters. Thermochim Acta. 1985;94:199–204.
35. Cingolani A, Berchiesi G, Franzosini P. Ternary system rubidium nitrate and silver nitrate and thallium nitrate. Gazz Chim Ital. 1971;101(12):981–9.
36. Liu J, Duan C-g, Ossowski MM, Mei WN, Smith RW, Hardy JR. Molecular dynamics simulation of structural phase transitions in $RbNO_3$ and $CsNO_3$. J Solid State Chem. 2001;160:222–9.
37. Pohl D, Gross T. Caesium nitrate (II) at 296 K. Acta Cryst. 1993;C49:316–8.
38. Zamali H, Jemal M. Diagrammes de phases des systèmes binaires KNO_3–$CsNO_3$ et KNO_3–$NaNO_3$. J Therm Anal. 1994;41:1091–9.
39. Hellali D, Zamali H, Sebaoun A, Jemal M. Phase diagram of the $AgNO_3$–$CsNO_3$ system. J Therm Anal Calorim. 1999;57:569–74.
40. Palkin AP. Zh Russ Fiz Khim Obshch. 1928;60:317. (cited in book: Ernest M. L. Carl R.R. and Howard F.McM.: Phase diagrams for ceramists 1969 supplement. Compiled at the National Bureau of standards, Margie K. Reser, Editor. Copyright by the American Ceramic Society. USA;1969).
41. Bridgman PW. Polymorphic changes under pressure of the univalent nitrates. Proc Am Acad. 1916;151:581–625.
42. Mustajoki A. The specific heat of cesium nitrate in the temperature interval 50–450 °C as well as the heat of transition and heat of fusion. Ann Acad Sci Fenn A. 1957;6–7:1–12.
43. Maeso MJ, Largo J. The heat capacities of $LiNO_3$ and $CsNO_3$ from 350 to 700 K. Thermochim Acta. 1993;222:195–201.
44. Jriri J, Rogez J, Bergman C, Mathieu JC. Thermodynamic study of the condensed phases of $NaNO_3$, KNO_3 and $CsNO_3$ and their transitions. Thermochim Acta. 1995;266:147–61.
45. Bol'shakov KA, Pokrovskii BI, Plyushchev VE. Binary systems formed by alkali metal nitrates. Zh Neorg Khim. 1961;6(9):2120–5.
46. Bol'shakov KA, Pokrovskii BI, Plyushchev VE. Binary systems formed by alkali metal nitrates. Russ J Inorg Chem. 1961;6(9):1083–6.
47. Belaid Drira N, Zamali H, Jemal M. Diagramme de phases et propriétés thermodynamiques du liquide du système binaire $CsNO_3$–$NaNO_3$. J Soc Chim Tun. 2001;4(10):1269–78.
48. Flotow HE, O'Hare PAG, Boerio-Goates J. Heat capacity from 5 to 350 K and thermodynamic properties of cesium nitrate to 725 K. J Chem Thermodyn. 1981;13:477–83.
49. Tadashi A, Mineo K, Hiroshi T. Studies on heat storage V Specific heat of molten alkali nitrates. Nagoya Kogyo Gijutsu Shikensho Hokoku. 1980;29(2):25–30.
50. Protsenko AV, Protsenko PI, Eremina NN. Na, Cs // NO_2, NO_3 system. Zh Neorg Khim. 1971;16(7):2009–11.
51. Nurminskii NN, Diogenov GG. Ternary reciprocal system of potassium and caesium acetates and nitrates. Russ J Inorg Chem. 1960;5(9):1011–3.
52. Bakes M, Dupuy J, Guion J. Etude d'anomalies électroniques d'origine structural en sels fondus. C R Acad Sci Paris. 1963;256(11):2376–8.
53. Zamali H, Jemal M. Phase diagrams of binary systems: $AgNO_3$–KNO_3 and $AgNO_3$–$NaNO_3$. J Phase Equilib. 1995;16(3):235–8.
54. Jriri T. Contribution à l'étude thermodynamique des systèmes binaires et ternaires de nitrates alcalins. Thesis, Univ. of Aix-Marseille I, Marseille, France, 1994.